Asymmetric Fluorescence Quenching of Dual-Emissive Porphyrin-Containing Conjugated Polyelectrolytes for Naked-Eye Mercury Ion Detection

Zhen Fang, Kan-Yi Pu, and Bin Liu*

Department of Chemical and Biomolecular Engineering, National University of Singapore, 4 Engineering Drive 4, 117576, Singapore

Received August 19, 2008; Revised Manuscript Received September 27, 2008

ABSTRACT: A series of cationic porphyrin-containing conjugated polyfluoreneethynylenes (PFEs) are synthesized for mercury(II) detection. The incorporation of porphyrin into the PFE backbone offers dual emissive polyelectrolytes with both blue and red emission bands resulting from incomplete intramolecular energy transfer from the fluoreneethynylene segments to the porphyrin units. In the presence of mercury(II), both blue emission from the fluoreneethynylene segments and red emission from the porphyrin units are quenched, and the quenching in red emission is significantly larger than that in blue emission. In the presence of other metal ions, for example, Zn^{2+}, Cu^{2+}, Cd^{2+}, Pd^{2+}, Co^{2+}, and Ni^{2+}, there is almost no change observed in red porphyrin emission, while the quenching in blue fluoreneethynylene emission is observed. The asymmetric quenching of the blue and red emission bands in the presence of various metal ions leads to real-time mercury(II) detection. Using a standard fluorometer, the fluorescence quenching of porphyrin for the best polymer has shown a linear response to mercury(II) in the concentration range of 0−100 μM, with a detection limit of 0.1 μM. In addition, the fluorescent color change of the polymer solution allows naked-eye detection of mercury(II) with a detection limit of 10 μM.

Introduction

Reliable technologies for detection of metal ions in environmental or biological systems are under extensive investigations.[1] Among heavy metal ion pollutants, mercury contamination is widespread and occurs through a variety of natural and anthropogenic sources.[2] Once the inorganic mercury is introduced into the marine environment, bacteria can convert it into methyl mercury. As a result, mercury enters the food chain and accumulates in human bodies, ultimately leading to human diseases.[3−5] Traditional mercury detection techniques include atom absorption spectroscopy,[6] induced coupled-plasma spectroscopy,[7] X-ray fluorescence spectrometry,[8] and anodic stripping voltammetry.[9] These methods are time-consuming and require complicated instruments. Recently, methods based on the fluorescence change of small molecules,[10] polymers,[11] and nanoparticles[12] have been developed for mercury(II) detection. These fluorescent methods have shown distinct advantages, such as convenience, moderate to high sensitivity, and good selectivity.[13] To meet the requirements for mercury(II) detection in various environmental samples, fluorescent assays continue to be optimized in selectivity, sensitivity and operation.

Conjugated polymer (CP)-based fluorescent chemosensors have been successfully utilized for the detection of a variety of analytes ranging from ions,[14] explosives,[15] to biomolecules.[16] In comparison with small molecular fluorophores, the electron-delocalized backbone structures of CPs allow for more rapid and efficient intrachain and interchain exciton migrations, giving rise to enhanced signal outputs with high detection sensitivity.[17] By introducing specific ligands such as pyridine,[18] phenanthroline,[19] quinoline,[20] and dipyrrolylquinoxaline[21] to the polymer backbones or side chains, CPs have been widely used for metal ion detection. The ligand units serve as the analyte receptor that coordinates with metal ions to generate exciton traps to quench the polymer fluorescence. Consequently, the signal readout for these CP-based chemosensors originates from the polymer fluorescence quenching, and the selectivity is provided by specific recognition between the ligand and analyte. Although the polymer fluorescence quenching based protocol has been widely used for mercury(II) sensing, these polymers do not provide good opportunities for visualization of the detection. Development of a new generation of CPs for naked-eye detection of mercury(II) in real time is of particular interest due to its practical convenience.

Porphyrins and their derivatives have been proven useful in metal ion detection with high selectivity and sensitivity.[22] The four-nitrogen-containing macrocycle of porphyrin can selectively coordinate mercury(II) to quench its fluorescence.[23] Porphyrin and its derivatives were reported to act as both ion receptors and signaling fluorophores.[24] The low-energy emission of porphyrin indicates that it could be incorporated into high energy CPs to allow intramolecular energy transfer.[25] Although some porphyrin based conjugated polymers have been synthesized, there is no report on water-soluble porphyrin-containing CPs and their applications for metal ion detection.

In this contribution, we report a series of water-soluble porphyrin-containing CPs (structures shown in Figure 1) for naked-eye detection and quantification of mercury(II). The polymer design takes advantage of the low energy emission and selective coordination properties of porphyrin in conjugation with the light-harvesting properties of CPs. To conduct mercury(II) detection in aqueous media, cationic polyfluoreneethynylene (PFE) is chosen as the main scaffold in consideration of its good water solubility, blue fluorescence, and convenient synthesis. Energy transfer from the fluoreneethynylene segments (energy donor) to the porphyrin units (energy acceptor) is studied. The optical response of these PFEs toward different metal ions is investigated in details through the UV−vis absorption and photoluminescence (PL) measurements. Detection and quantification of mercury(II) using both fluorescence spectroscopy and naked eye is demonstrated.

Results and Discussion

Synthesis. Scheme 1 depicts the synthesis of a series of cationic poly(fluoreneethynylene)s with different porphyrin molar contents. 2,7-Dibromo-9,9′-bis(6-bromohexyl)fluorene

* To whom correspondence should be addressed. E-mail: cheliub@nus.edu.sg.

10.1021/ma801874z CCC: $40.75
Published on Web 10/28/2008

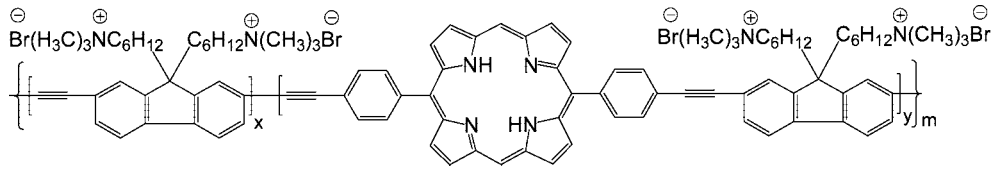

Figure 1. Structure of porphyrin-containing polyfluoreneethynylene.

Scheme 1. Synthetic Route to CCPs[a]

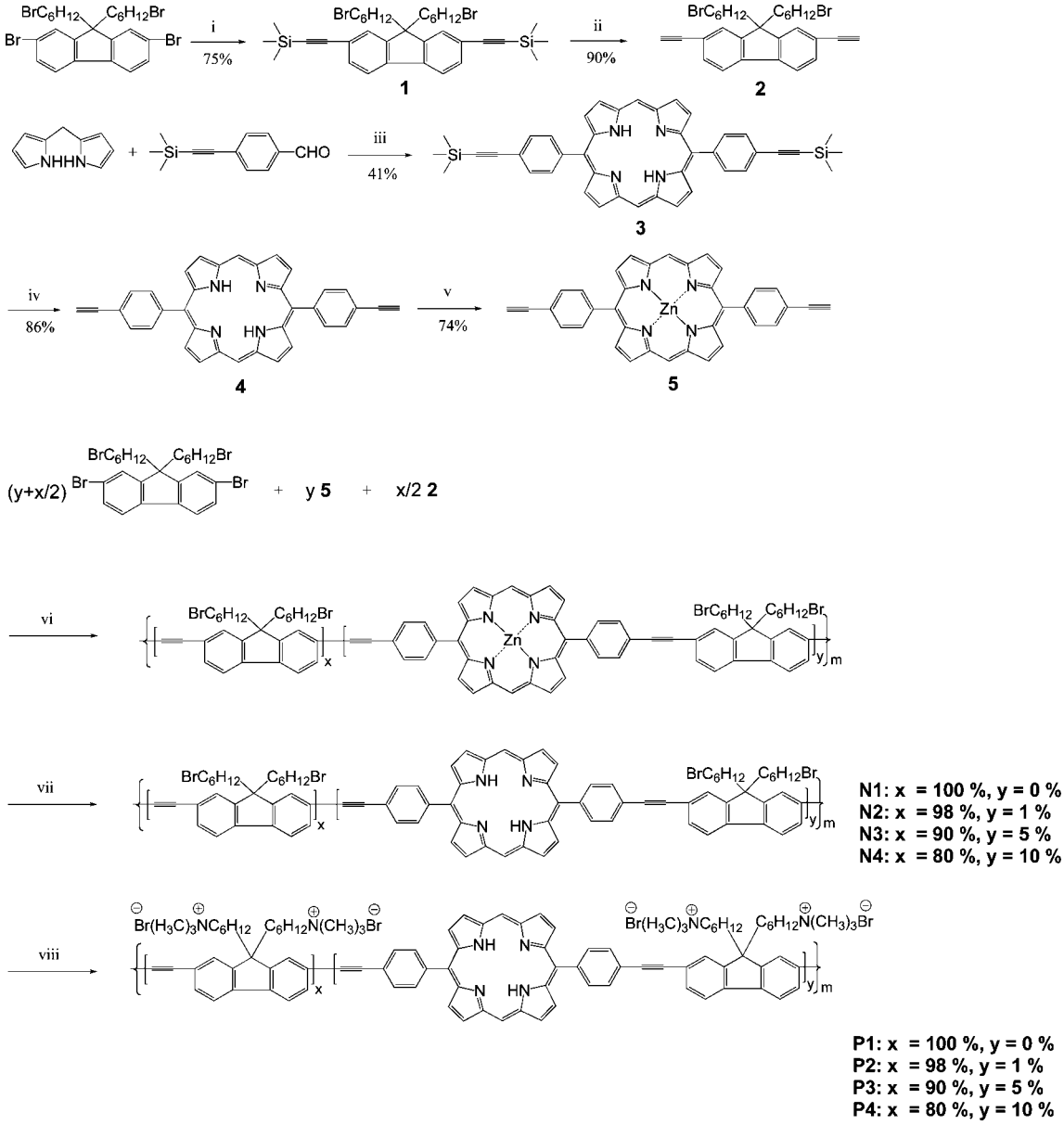

[a] Reagents and conditions: (i) $(Ph_3P)_2PdCl_2$, CuI, trimethylsilylacetylene, triethylamine, 6 h, N_2, 70 °C; (ii) KOH, THF, MeOH, H_2O, 1 h; (iii) CH_2Cl_2, trifluoroacetic acid, 15 h, N_2, room temperature; chloranil, 50 °C, 1 h; (iv) KOH, THF, MeOH, H_2O, 2 h; (v) $Zn(CH_3COO)_2$, $CHCl_3$, CH_2Cl_2, MeOH, 12 h; (vi) $(Ph_3P)_4Pd$, CuI, diisopropylamine, THF, 10 h, N_2, 70 °C; (vii) trifluoroacetic acid, CH_2Cl_2, 12 h; (viii) trimethylamine, THF, −78 °C to room temperature, 12 h; MeOH, 24 h.

was synthesized according to our previous report.[26] Coupling between 2,7-dibromo-9,9′-bis(6-bromohexyl)fluorene and trimethylsilylacetylene under a typical Sonogashira condition afforded 2,7-ditrimethylsilylethynyl-9,9′-bis(6-bromohexyl) fluorene (**1**) in 75% yield. After removal of the trimethylsilyl groups in KOH/THF/MeOH solution, the monomer 2,7-diethynyl-9,9′-bis(6-bromohexyl)fluorene (**2**) was obtained in 90% yield. 5,15-*p*-Trimethylsilylethynylphenyl porphyrin (**3**) was prepared in 41% yield from dipyrromethane and 4-(2-(trimethylsilyl)ethynyl)benzaldehyde through a modified MacDonald condensation followed by recrystallization from chloroform and hexane.[27,28] The original attempt to copolymerize 2,7-dibromo-9,9′-bis(6-bromohexyl)fluorene, **2**, and **4** resulted in red insoluble solids, which was caused by Pd(II)-accelerated coordination between copper ions (from the catalyst) and porphyrin.[29,30] To avoid porphyrin aggregation, an alternative method was carried out to coordinate the monomer porphyrin **4** with zinc(II) first, which was followed by polymerization and demetalation in the

last step (Scheme 1). The metalation process was monitored by measuring the UV−vis absorption spectra of the reaction solution. Upon formation of metalloporphyrin **5**, the four absorption Q-bands near 500∼700 nm for metal free porphyrin reduced to two. Meanwhile, the resonance signal at $\delta = -3.13$ ppm for the two central protons of porphyrin **4** disappeared in the ^{1}H NMR spectrum.

The neutral precursor polymers were synthesized through adjusting the feed ratio of monomers **2**, **5**, and 2,7-dibromo-9,9′-bis(6-bromohexyl) fluorene, which contain 0, 1, 5, and 10 mol % of zincporphyrin, respectively. The obtained polymers were then dissolved in $CHCl_3$ and stirred overnight at room temperature in the presence of trifluoroacetic acid to remove zinc(II). The UV−vis spectroscopy was used to monitor the dissociation of zinc(II) from the porphyrin cycles. Upon demetalation, the two absorption Q-bands for metalloporphyrin recovered to four. Polymers **N1**, **N2**, **N3**, and **N4** (Scheme 1) were obtained as yellow, brown, purple, and red powders with yields of ∼80−90%.

The structures of these neutral polymers were affirmed by NMR spectra. The ^{1}H and ^{13}C NMR spectra of **N2** are similar to those of **N1**. Due to the low feed ratio of porphyrin for **N2**, the resonances of Hs and Cs for the porphyrin cycles are undetectable. The ^{1}H NMR spectrum of **N3** shows resonance signals at $\delta = 10.37$, 9.49, and 9.18 ppm, corresponding to the protons of porphyrin. The ratio of the integrated areas for protons of porphyrin to those of fluorene units indicates that **N3** and **N4** contain approximately 4.5 and 9.1 mol % of porphyrin, respectively. Polymers **N1**−**N4** have number average molecular weights of 15000, 12000, 9000, and 5000, with polydispersities of 2.2, 2.5, 2.6, and 3.2, respectively. With the increased porphyrin feed ratio, the polymer molecular weight decreases due to the relatively low reactivity of **5** as compared to that of **2**, and the reduced polymer solubility in THF with increased porphyrin content.

Cationic conjugated polymers (CCPs) **P1**−**P4** were synthesized through amination of the corresponding neutral precursor polymers **N1**−**N4** in THF by addition of trimethylamine. The chemical structures of **P1**−**P4** were affirmed by NMR spectra. For each CCP, the ratio of the integrated areas for $-C\underline{H}_2Br$ and $-CH_2N(C\underline{H}_3)_3$ in the ^{1}H NMR spectra indicates that the degree of quaternization is higher than 95%. We failed to obtain the ^{13}C NMR spectra for both **P3** and **P4** due to their limited solubility (<5 mg/mL in CD_3OD).

Optical Properties. To study the effect of porphyrin content on the overall optical properties of CCPs, the absorption and emission spectra of **P1**−**P4** in water at a fixed repeat unit concentration ([RU] = 1 μM) were measured (Figure 2). Here RU is defined as the repeat unit, for example, 1 mol RU of **P2** includes 0.01 mol of porphyrin units and 0.99 mol of fluorene-ethynylene units. As shown in Figure 2a, **P1** has a maximum absorption at 388 nm with a minor absorption peak at 411 nm. With the increased porphyrin content in the polymer backbone, a gradual increase in intensity for the absorption band at ∼411 nm was observed for **P2**, **P3**, and **P4**, as a result of contribution from the S_0-S_2 transition of porphyrin at ∼411 nm.[22] The absorption of Q-bands at 500∼700 nm (attributed to S_0-S_1 transition of porphyrin) was clearly found for **P3** and **P4**, while it was invisible for **P2** due to the low feed ratio of porphyrin units.

As shown in Figure 2b, **P1**−**P4** have a similar emission band in the blue region, with a maximum at 423 nm and a shoulder at ∼445 nm. In addition, **P2**, **P3**, and **P4** have additional emission bands at 600−700 nm, corresponding to the porphyrin units. The overall quantum yield was measured to be 35% for **P1**, 27% for **P2**, 22% for **P3**, and 13% for **P4**, respectively, for both blue and red emission. Despite the cationic nature of

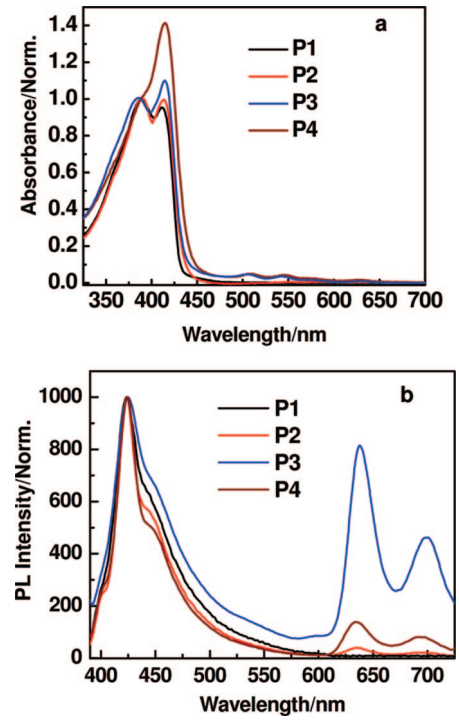

Figure 2. Normalized absorption (**a**, normalized at 388 nm) and emission (**b**, normalized in the blue region) of **P1**−**P4** in water. λ_{ex} = 375 nm, [RU] = 1 μM.

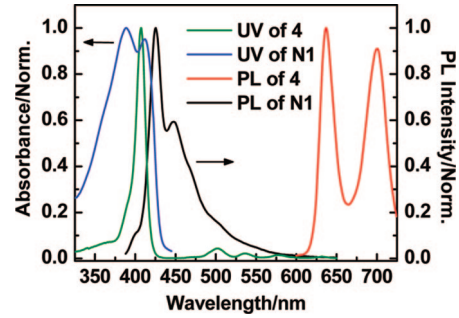

Figure 3. Normalized absorption and emission spectra of monomer **4** and **N1** in THF: [**4**] = 1 μM = [RU] for **N1**; excitation at 407 nm for **4** and 390 nm for **N1**.

P2−**P4**, $\pi-\pi$ stacking of porphyrin units could overcome the electrostatic repulsive force, resulting in porphyrin aggregation[31] and a decrease in the quantum yield of the polymers. In addition, the relative porphyrin emission intensity for **P2**−**P4** also changes with the porphyrin content. When excited at 375 nm, **P2** emits very weak fluorescence at the porphyrin emission band. The highest porphyrin emission is observed for **P3**, which has 4.5 mol % porphyrin units, and the porphyrin emission from **P4** (9.1 mol % porphyrin content) is only slightly higher than that of **P2**. The increased porphyrin content in the polymer on the one hand increases the porphyrin emission intensity through energy transfer,[32] on the other hand, induces more self-aggregation of porphyrin and reduces the charge density of the polymers, which are detrimental to the porphyrin emission intensity.[33] The balance of these factors leads to the highest porphyrin emission for **P3** in water.

Energy Transfer Study. Figure 3 shows the normalized absorption and emission spectra of **N1** and porphyrin **4** in THF. Compound **4** has a narrow absorption band centered at 407 nm with relatively weak Q-bands from 500 to 650 nm, which overlap with the emission of **N1**. Accordingly, energy transfer from PFE to porphyrin is anticipated. Figure 4 shows the

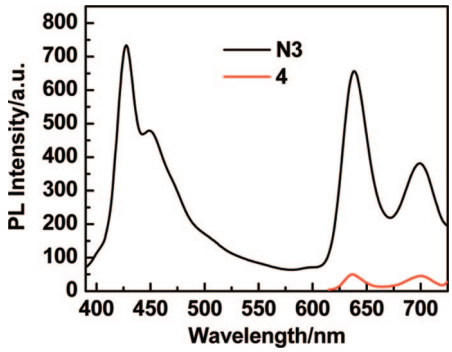

Figure 4. Emission spectra of **N3** and monomer **4** in THF: excitation at 375 nm; [porphyrin] in **N3** = [**4**] = 0.05 μM.

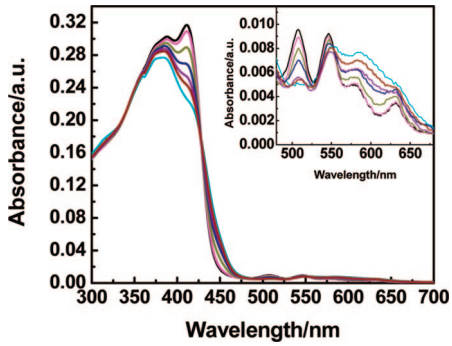

Figure 5. Absorption spectra of **P3** in water upon addition of Hg^{2+}: [RU] = 10 μM; [Hg^{2+}] = 0, 10, 30, 50, 80, 100, and 300 μM.

emission spectra of **4** and **N3** upon excitation at 375 nm. Here, 375 nm is selected as the excitation wavelength because there is no significant absorption for **4** at this wavelength (Figure 3). The emission of **4** is relatively weak compared to that of **N3** in the region of 600−700 nm, while the porphyrin unit concentration in both solutions is maintained identical ([porphyrin] in **N3** = [**4**] = 0.05 μM). This result indicates that energy transfer could occur between fluoreneethynylene segments and porphyrin units.

Effect of Metal Ions on Absorption Spectra. Figure 5 shows the effect of mercury(II) on the absorption spectra of **P3**. In the absence of mercury(II), **P3** has a maximum absorption at 411 nm responsible for both porphyrin and fluoreneethynylene segments, and a minor absorption peak at 388 nm corresponding to fluoreneethynylene units. Upon addition of mercury(II), the absorption band at 411 nm decreases in intensity, which is concomitant with a red-shifted onset absorption from 445 to 475 nm. These changes are due to the complexation of mercury(II) to porphyrin, and the metalloporphyrin absorbs at a longer wavelength with a smaller extinction coefficient as compared to that of metal-free porphyrin.[34] Meanwhile, the four Q-bands reduce to two bands upon addition of mercury(II), which also verifies the formation of metalloporphyrin.[35] It is well-known that upon introduction of mercury(II) into the porphyrin center, the symmetry of the macrocycle increases so that the transformation from D_{2h} to C_{4v} (or D_{4h}) occurs, resulting in a reduced number of S_1 and S_2 vibronic levels and a decrease in the number of Q-bands.[35]

The effect of other metal ions on the absorption spectra of **P3** was also examined. The changes in the absorption spectra of **P3** upon addition of Cu^{2+} are shown in Figure 6. Insignificant changes are found either for the band at 411 nm or for the four Q-bands. Other metal ions, including Cd^{2+}, Pb^{2+}, Ni^{2+}, Co^{2+}, and Zn^{2+} show similar trends as that of Cu^{2+} (Figures S1−S5 in the Supporting Information), which indicate that the non-specific ions are rather difficult to complex with the porphyrin

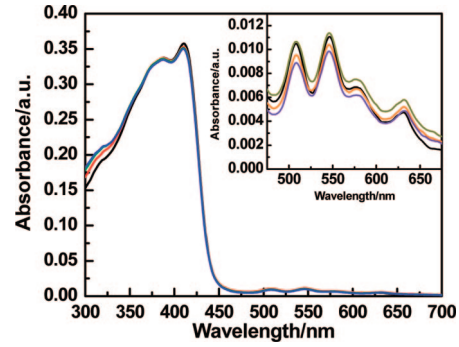

Figure 6. Absorption spectra of **P3** in water at [RU] = 10 μM in the presence of Cu^{2+} with concentrations ranging from 0, 10, and 100−1000 μM.

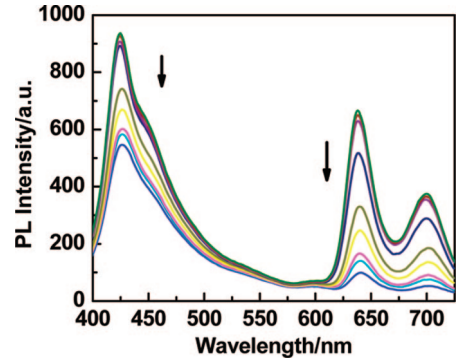

Figure 7. Changes in emission spectra of **P3** upon addition of Hg^{2+}: [RU] = 1 μM; [Hg^{2+}] = 0, 0.1, 1, 10, 30, 50, 80, 100, and 300 μM; excitation at 388 nm.

units in **P3**. As a consequence, good selectivity of mercury(II) over other ions is demonstrated for **P3**.

Ion-Induced Fluorescence Quenching. To study the effect of different metal ions (Hg^{2+}, Cu^{2+}, Zn^{2+}, Cd^{2+}, Pb^{2+}, Co^{2+}, Ni^{2+}) on the fluorescence property of **P3**, the effect of these ions on the fluorescence property of polyfluoreneethynylene (**P1**) was studied first. Experiments were carried out at a fixed [RU] = 1 μM. Upon addition of the metal ions, the fluorescence of **P1** gradually decreases. With the metal ion concentration increased from 0 to 25 μM, the fluorescence quenching of **P1** conforms to the Stern−Volmer equation $I_0/I = K_{sv}[\text{ion}] + 1$,[36] where I_0 and I represent the **P1** fluorescence intensities in the absence and presence of metal ions, respectively. K_{sv} is the Stern−Volmer constant, which provides a quantitative measure of quenching efficiency. The K_{sv} values for **P1** are in the range of 2.4−3.1 × 10^3 M^{-1} for Hg^{2+}, Cu^{2+}, Pb^{2+}, Ni^{2+}, Co^{2+}, and Zn^{2+}, respectively (shown in Figure S6 in the Supporting Information). Addition of Na^+ to **P1** solution also results in fluorescence quenching with a K_{sv} of ∼1.5 × 10^3 M^{-1}, which indicates that the quenching is largely due to the increased ionic strength in solution. We notice that the K_{sv} (4.9 × 10^3 M^{-1}) of Cd^{2+} is slightly larger than that of other ions. However, the reason for such a difference awaits further investigation. These data illustrate that, in the absence of the porphyrin units, the homopolymer (**P1**) almost has no selectivity for metal ions.

To examine the role of porphyrin in metal ion detection, similar titration experiments were performed for **P3**. Figure 7 shows the effect of mercury(II) on the fluorescence of **P3** in aqueous solution. With the addition of mercury(II), the blue emission at 425 nm decreases gradually and the shoulder near 450 nm disappears. The quenching of blue emission from the fluoreneethynylene segments is similar to that observed for **P1**. However, the porphyrin emission shows a noticeable response to Hg^{2+}, and the emission bands at 600−700 nm decrease with

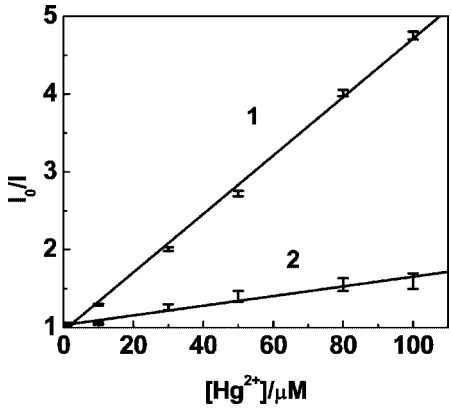

Figure 8. Relative fluorescence intensity I_0/I of **P3** vs $[Hg^{2+}]$. **1**: based on red emission from porphyrin units; **2**: based on blue emission from fluoreneethynylene segments; excitation at 388 nm.

increased $[Hg^{2+}]$. At $[Hg^{2+}] = 300\ \mu M$, the red porphyrin fluorescence is almost completely quenched, while the blue fluorescence of fluoreneethynylene segments is more than half of its initial. This fluorescence quenching is consistent with the effect of mercury(II) on the absorption spectra of **P3** (Figure 5). The asymmetric quenching of mercury(II) for blue and red emission bands indicates that the K_{sv} for mercury(II) quenching of fluoreneethynylene and porphyrin units is different. As shown in Figure 8, I_0 and I represent the fluorescence intensities of either fluoreneethynylene or porphyrin emission upon excitation at 388 nm in the absence and presence of mercury(II), respectively. The K_{sv} value for quenching of fluoreneethynylene segments is calculated to be $6.2 \times 10^3\ M^{-1}$, which is in the same order as that for **P1**. The K_{sv} value for quenching of porphyrin units is approximately $4.0 \times 10^4\ M^{-1}$, which is over 6-fold higher than that for fluoreneethynylene segments. At $[Hg^{2+}] = 300\ \mu M$, the fluorescent color of the polymer solution ($[RU] = 1\ \mu M$) is blue, which is different from the initial purple blank solution.

To understand the fluorescence quenching of **P3** upon addition of Hg^{2+}, the fluorescence change of porphyrin was monitored upon excitation at 546 and 375 nm, respectively. These two wavelengths were chosen because the fluoreneethynylene segment in **P3** does not have absorption at 546 nm (Q-band), and the porphyrin does not have significant absorption at 375 nm. As a consequence, upon excitation at 546 nm, no energy transfer occurs in solution and the decreased porphyrin fluorescence is due to prophyrin quenching upon porphyrin-Hg^{2+} complexation. The I_0/I versus $[Hg^{2+}]$ upon excitation at both wavelengths are shown in Figure S7 in the Supporting Information. It is found that the porphyrin emission quenching rate upon excitation at 375 nm is only slightly higher than that upon excitation at 546 nm, which indicates that the prophyrin$-Hg^{2+}$ complexation induced fluorescence quenching plays a dominant role in the observed fluoresce decrease in red emission, and the energy transfer process does not significantly amplify this quenching.

To study the influence of other metal ions on the fluorescence of **P3**, experiments were carried out under similar conditions to that for Hg^{2+}. The results are shown in Figures S8$-$S12 in the Supporting Information. Figure 9 shows the changes in emission spectra of **P3** upon addition of Cu^{2+}. With increased $[Cu^{2+}]$, the blue emission of fluoreneethynylene segments is quenched gradually, which is similar to that in the presence of Hg^{2+}. The quenching of fluoreneethynylene segments is also observed when Cd^{2+}, Pb^{2+}, Ni^{2+}, Co^{2+}, and Zn^{2+} are used for titration. However, these metal ions do not quench the red emission of porphyrin units obviously (Figures S7$-$S11 in the Supporting Information), which suggests that there is almost no metalloporphyrin formation in the presence of nonspecific

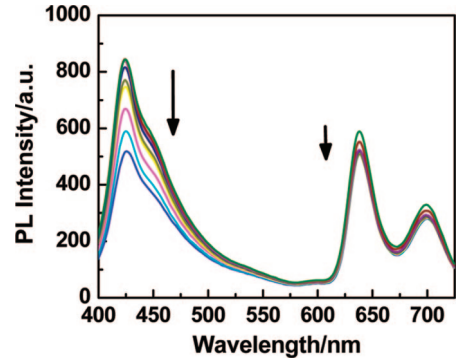

Figure 9. Changes in emission spectra of **P3** upon addition of Cu^{2+}: $[RU] = 1\ \mu M$; $[Cu^{2+}] = 0$, 0.1, 1, 10, 30, 50, 80, 100, and 300 μM; excitation at 388 nm.

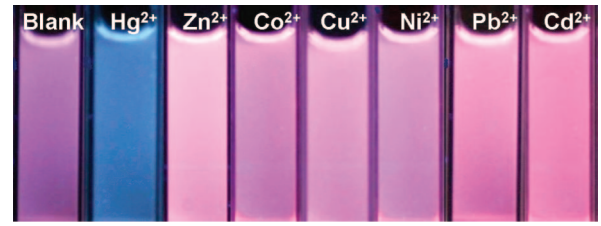

Figure 10. Photographs of **P3** solution at $[RU] = 10\ \mu M$ in the presence of 1000 μM various ions under a hand-held UV-lamp with $\lambda_{max} = 365$ nm.

metal ions except for mercury(II) at the studied metal ion concentration range. We also notice that the quenching of fluoreneethynylene segments for **P3** in the presence of Cd^{2+} (Figure S8 in the Supporting Information) is also slightly larger than that in the presence of other ions, which agrees with the observation for fluorescence quenching of **P1** by Cd^{2+} (Figure S6 in the Supporting Information).

Mercury Quantification. Relied on the preferred fluorescence quenching of the porphyrin units in the presence of mercury(II) over other metal ions, detection and quantification of mercury(II) in aqueous solution is feasible. For 1:1 porphyrin mercury complex, the overall equilibrium could be described using eq 1[37]

$$H_2P + Hg^{2+} \overset{K}{\rightleftharpoons} HgP + 2H^+ \quad (1)$$

$$K = \frac{[HgP][H^+]^2}{[H_2P][Hg^{2+}]} \quad (2)$$

where, H_2P and HgP represent a free base porphyrin and its metal complex, respectively, and K is the equilibrium constant of the reaction. The relationship between the relative intensity and Hg^{2+} concentration is expressed as the quenching equation ($I_0/I = K_{sv}[Hg^{2+}] + 1$) in dilute solution. Figure 8 shows that the relative fluorescence intensity of porphyrin has a linear relation versus $[Hg^{2+}]$ ranging from 0.1 to 100 μM. This linear response could serve as a calibration curve for determination of mercury concentration. The limit of detection (LOD) is estimated to be approximately 0.1 μM.

Naked-Eye Detection of Metal Ions. Figure 10 shows the photographs of **P3** in the presence of different metal ions under a hand-held UV-lamp with $\lambda_{max} = 365$ nm. At $[Hg^{2+}] = 1000$ μM, the red porphyrin emission is completely quenched and the fluorescent color of the polymer solution is bright blue. The polymer solution appears pink or purple in the presence of other metal ions at the equal concentration of mercury(II), because only the fluorescence from the fluoreneethynylene segments is

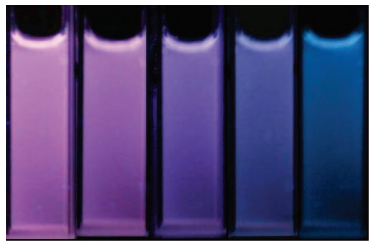

Figure 11. Photographs of **P3** solution at [RU] = 10 μM with [Hg^{2+}] ranging from 0, 10, 100, and 500−1000 μM from left to right under a hand-held UV-lamp with λ_{max} = 365 nm.

partially quenched. The change in fluorescent color for **P3** in the presence of different metal ions highlights the feasibility of naked-eye detection of mercury(II). In addition, with increased [Hg^{2+}], the fluorescent color of **P3** solution gradually transfers from purple to blue (Figure 11), which allows naked-eye mercury quantification with a detection limit of 10 μM. This is among the lowest visual detection limits obtained for CP-based mercury(II) sensors in aqueous solution.[14]

Conclusions

In summary, we have demonstrated a new asymmetric fluorescence quenching concept for multicolor sensing of mercury(II) in aqueous solution. This method relies on CPs containing a small fraction of porphyrin units to act as both an energy acceptor and a metal ion recognition element. A series of porphyrin-containing cationic PFEs were synthesized through a new synthetic approach by Sonogashira coupling polymerization between 2,7-dibromo-9,9′-bis(6-bromohexyl)fluorene, **2** and Zn(II) coordinated porphyrin, which was followed by demetalation. Upon excitation of the fluoreneethynylene segments at 375 nm, the polymer with 4.5 mol % porphyrin units showed strong emission at both the blue and the red region, as a result of intramolecular energy transfer from the fluoreneethynylene segments to the porphyrin units. It was found that mercury(II) could quench the red porphyrin emission efficiently and the quenching gave a linear response to mercury(II) in the concentration range of 0−100 μM, with a detection limit of 0.1 μM using a standard fluorometer. In addition, mercury(II) could quench the emission from porphyrin units more efficiently than that from fluoreneethynylene segments, which caused the solution fluorescent color to change from purple to blue in the presence of mercury(II). In the presence of other metal ions, such as Cu^{2+}, Cd^{2+}, Pb^{2+}, Ni^{2+}, Co^{2+}, and Zn^{2+}, only slight quenching in the fluoreneethynylene segments was observed, and the solution fluorescent color appeared pink or purple. The asymmetric fluorescence quenching of the porphyrin containing polymer provided an opportunity to detect mercury(II) in real time by naked eye with a detection limit of 10 μM. This study opens up new opportunities for designing CP-based multicolor fluorescent chemosensors.

Experimental Section

All chemical reagents were purchased from Sigma-Aldrich Chemical Co., and were used as received. Dichloromethane for porphyrin synthesis was refluxed over calcium hydride. Other solvents (AR grade) were used without further purification. Dipyrromethane was synthesized according to the literature.[29] 2,7-Dibromo-9,9′-bis(6-bromohexyl)fluorene was synthesized according to our previous method.[26] The stock mercury(II) solution (1 M) was prepared by dissolving 1.59 g $Hg(CH_3COO)_2$ in 5 mL of water with the addition of 2 drops of concentrated nitric acid. The stock solution was further diluted to different concentrations for measurement. Other metal ion solutions were prepared using the same procedure.

The NMR spectra were collected on a Bruker DPX 300, 400, or 500 spectrometer with chloroform-*d* and methanol-d_4 as the solvent. EI-mass analysis and elemental analysis were carried out by the Chemical Molecular and Materials Analysis Centre (CMMAC) of the National University of Singapore. GPC analysis was conducted with a Waters 2690 liquid chromatography system equipped with Waters 996 photodiode detector and Phenogel GPC columns, using polystyrenes as the standard and THF as the eluent at a flow rate of 1.0 mL/min at 35 °C. The UV−vis absorption spectra were recorded on a SHIMAZU UV−vis 1770 spectrometer. The emission spectra were recorded on a Perkin-Elmer LS55 fluorometer. Photographs of the polymer solutions were taken using a Canon EOS 400D Digital camera under a hand-held UV-lamp with λ_{max} = 365 nm.

9,9′-Bis(6-bromohexyl)-2,7-[bis(2-trimethysilyl)ethynyl)]fluorene (1). A solution of trimethylsilyl acetylene (1.08 g, 1.55 mL, 11.0 mmol, d = 0.695 g/mL) in diisopropylamine (20.0 mL) was slowly added to a solution of 2,7-dibromo-9,9′-bis(6-bromohexyl)fluorene (3.25 g, 5.0 mmol), $(Ph_3P)_2PdCl_2$ (0.175 g, 0.25 mmol), and CuI (0.047 g, 0.25 mmol) in diisopropylamine (50.0 mL) under nitrogen at room temperature. The reaction mixture was then stirred at 70 °C for 8 h. The solvent was removed under reduced pressure, and the residue was chromatographed on silica gel using hexane as eluent to give **1** (2.5 g, 75%) as white crystals. ^{1}H NMR (300 MHz, $CDCl_3$, δ, ppm): 7.60 (d, 2H, J = 7.8 Hz), 7.46 (dd, 2H, J = 1.2 Hz, J = 7.8 Hz), 7.40 (s, 2H), 3.28 (t, 4H, J = 6.8 Hz), 1.97−1.91 (m, 4H), 1.70−1.60 (m, 4H), 1.22−1.00 (m, 8H), 0.62−0.44 (m, 4H), 0.29 (s, 18H). ^{13}C NMR (75 MHz, $CDCl_3$, δ, ppm): 150.53, 140.79, 131.34, 126.10, 121.88, 119.89, 105.89, 94.46, 55.07, 40.14, 33.84, 32.64, 28.99, 27.79, 23.39, 0.02. Anal. Calcd for $C_{35}H_{48}Br_2Si_2$: C, 61.39; H, 7.07. Found: C, 61.40; H, 7.00. MS (EI): m/z 683.96.

9,9′-Bis(6-bromohexyl)-2,7-diethynylfluorene (2). A KOH aqueous solution (6.0 mL, 20.0%) was diluted with methanol (25.0 mL) and added to a stirred solution of **1** (3.42 g, 5.0 mmol) in THF (50.0 mL). The mixture was stirred at room temperature for 1 h and extracted with hexane. The organic fraction was washed with water and dried over sodium sulfate. The crude product was chromatographed on silica gel using hexane as the eluent. Recrystallization of the product from methanol gave **2** (2.7 g, 90%) as white crystals. ^{1}H NMR (300 MHz, $CDCl_3$, δ, ppm): 7.60 (d, 2H, J = 7.8 Hz), 7.45 (dd, 2H, J = 1.3 Hz, J = 7.8 Hz), 7.41 (s, 2H), 3.24 (t, 4H, J = 6.8 Hz), 3.12 (s, 2H), 1.98−1.85 (m, 4H), 1.68−1.57 (m, 4H), 1.20−0.96 (m, 8H), 0.60−0.45 (m, 4H). ^{13}C NMR (75 MHz, $CDCl_3$, δ, ppm): 150.65, 140.95, 131.39, 126.43, 120.97, 120.06, 84.38, 77.52, 55.07, 40.06, 33.82, 32.62, 28.99, 27.77, 23.37. Anal. Calcd for $C_{29}H_{32}Br_2$: C, 64.46; H, 5.97. Found: C, 64.23; H, 5.97. MS (EI): m/z 540.20.

5,15-(*p*-Trimethylsilylethynylphenyl) Porphyrin (3). A solution containing dipyrromethane (0.50 g, 3.4 mmol) and 4-trimethylsilylethynylbenzaldehyde (0.69 g, 3.4 mmol) in anhydrous CH_2Cl_2 (250 mL) was bubbled with nitrogen for 0.5 h. A total of 3 drops of trifluoroacetic acid were added. The solution was stirred at room temperature for 15 h under nitrogen. After 3.5 g chloranil was added, the mixture was refluxed for 1 h. After the solvent was removed, the crude product was purified over silica gel using 1:1 hexane/CH_2Cl_2 as the eluent. Further purification was carried out by continuous extraction of the crude product with methanol for 12 h to yield **3** (0.45 g, 41%) as a purple solid. ^{1}H NMR (500 MHz, $CDCl_3$, δ, ppm): 10.31 (s, 2H), 9.40 (d, 4H, J = 5.0 Hz), 9.05 (d, 4H, J = 4.5 Hz), 8.22 (d, 4H, J = 8.0 Hz), 7.93 (d, 4H, J = 8.0 Hz), 0.41 (s, 18H), −3.15 (s, 2H); ^{13}C NMR (125 MHz, $CDCl_3$, δ, ppm): 146.91, 145.28, 141.64, 140.63, 134.69, 131.87, 130.82, 130.63, 122.68, 118.36, 105.52, 95.66, 0.09. Anal. Calcd for $C_{42}H_{38}N_4Si_2$: C, 77.02; H, 5.85; N, 8.55. Found: C, 76.96; H, 5.68; N, 8.51. MS (EI): m/z 654.50.

5,15-(*p*-Ethynylphenyl) Porphyrin (4). To a solution of **3** (0.13 g, 0.2 mmol) in THF (100 mL), a solution of KOH (2 mL, 20%) diluted with methanol (30 mL) was added. After the mixture was stirred at room temperature for 2 h, it was extracted with CH_2Cl_2 and washed with water. After drying over Na_2SO_4, the solvent was

distilled out. The crude product was purified over silica gel using 1:1 hexane/CH_2Cl_2 as the eluent to yield **4** (0.87 g, 86%) as a purple solid. ^{1}H NMR (500 MHz, $CDCl_3$, δ, ppm): 10.34 (s, 2H), 9.41 (d, 4H, J = 4.4 Hz), 9.06 (d, 4H, J = 4.5 Hz), 8.25 (d, 4H, J = 8.2 Hz), 7.95 (d, 4H, J = 8.2 Hz), 3.35 (s, 2H), −3.13 (s, 2H). Anal. Calcd for $C_{36}H_{22}N_4$: C, 84.68; H, 4.34; N, 10.97. Found: C, 84.38; H, 4.23; N, 10.76. MS (EI): m/z 510.30.

5,15-(*p*-Ethynylphenyl) Zincporphyrin (5). To a solution of **4** (0.055 g, 0.1 mmol) in $CH_2Cl_2/CHCl_3$ (20 mL, 1:1), a suspension of $Zn(CH_3COO)_2 \cdot 2H_2O$ (0.12 g, 0.55 mmol) in 1 mL of methanol was added. The reaction was monitored by UV absorbance. After the mixture was stirred at room temperature for 12 h, it was washed with water and 10% Na_2CO_3, and then dried over Na_2SO_4. After the solvent was distilled out, the crude product was purified over silica gel using 1:2 hexane/CH_2Cl_2 as the eluent to yield **5** (0.041 g, 74%) as a purple solid. ^{1}H NMR (500 MHz, $CDCl_3$, δ, ppm): 10.30 (s, 2H), 9.42 (s, 4H), 9.09 (s, 4H), 8.23 (2, 4H), 7.93 (s, 4H), 3.34 (s, 2H). Anal. Calcd for $C_{36}H_{20}N_4Zn$: C, 75.33; H, 3.51; N, 9.76. Found: C, 75.01; H, 3.61; N, 9.46. MS (EI): m/z 573.40.

Poly[9,9′-bis(6-bromohexyl-fluorene)ethynylene] (N1). A solution of 2,7-dibromo-9,9′-bis(6-bromohexyl)fluorene (0.073 g, 0.112 mmol) and diethynylfluorene **2** (0.060 g, 0.112 mmol) in 4 mL of diisopropylamine/THF (1:3) was bubbled with nitrogen for 0.5 h. $Pd(PPh_3)_4$ (2.4 mg, 0.003 mmol) and CuI (0.5 mg, 0.002 mmol) were added. The mixture was stirred at 70 °C under nitrogen protection for 12 h and precipitated into 100 mL of methanol. The polymer was filtered and washed with methanol and acetone, and then dried under vacuum for 24 h to yield **N1** (0.102 g, 85%) as a yellow solid. ^{1}H NMR (300 MHz, $CDCl_3$, δ, ppm): 7.72−7.44 (m, 6H), 3.32−3.30 (m, 4H), 2.00 (br, 4H), 1.68 (br, 4H), 1.22 (br, 4H), 1.11 (br, 4H), 0.62 (br, 4H); $M_n = 1.5 \times 10^4$, $M_w/M_n = 2.2$.

N2−**N4** were synthesized using a similar procedure as that for the synthesis of **N1**.

N2. 2,7-Dibromo-9,9′-bis(6-bromohexyl)fluorene (0.073 g, 0.112 mmol), diethynylfluorene **2** (0.059 g, 0.110 mmol), zincporphyrin **5** (1.3 mg, 0.002mmol), $Pd(PPh_3)_4$ (2.4 mg, 0.003 mmol), and CuI (0.5 mg, 0.002 mmol) were stirred at 70 °C for 12 h and precipitated into methanol to afford an orange solid (0.095 g, 79%). The obtained polymer (0.052 g) was dissolved in CH_2Cl_2 (35 mL), and trifluoroacetic acid (1.5 mL) was added slowly. The mixture was stirred at room temperature for 12 h and precipitated into methanol to yield **N2** (0.045 g, 90%) as a brown solid. ^{1}H NMR (300 MHz, $CDCl_3$, δ, ppm): 7.72−7.44 (m, 6H), 3.31 (m, 4H), 2.02 (br, 4H), 1.68 (br, 4H), 1.21−1.11 (br, 4H), 0.62 (br, 4H); $M_n = 1.2 \times 10^4$, $M_w/M_n = 2.5$.

N3. 2,7-Dibromo-9,9′-bis(6-bromohexyl)fluorene (0.073 g, 0.112 mmol), diethynylfluorene **2** (0.055 g, 0.101 mmol), and zincporphyrin **5** (6.5 mg, 0.011mmol) were polymerized using $Pd(PPh_3)_4$ (2.4 mg, 0.003 mmol) and CuI (0.5 mg, 0.002 mmol) as the catalyst, which was followed by treatment with trifluoroacetic acid to yield **N3** (0.101 g, 80%) as a purple solid. ^{1}H NMR (500 MHz, $CDCl_3$, δ, ppm): 10.37 (br), 9.49 (br), 9.17 (m), 8.28 (br), 8.03 (br), 7.68−7.47 (m), 3.30 (s), 1.99 (br), 1.68 (br), 1.21 (br), 1.11 (br), 0.63 (m); $M_n = 9.0 \times 10^3$, $M_w/M_n = 2.6$.

N4. 2,7-Dibromo-9,9′-bis(6-bromohexyl)fluorene (0.073 g, 0.112 mmol), diethynylfluorene **2** (0.049 g, 0.090 mmol), and zincporphyrin **5** (13 mg, 0.023mmol) were polymerized using $Pd(PPh_3)_4$ (2.4 mg, 0.003 mmol) and CuI (0.5 mg, 0.002 mmol) as the catalyst, which was followed by treatment with trifluoroacetic acid to yield **N4** (0.105 g, 85%) as a red solid. ^{1}H NMR (500 MHz, $CDCl_3$, δ, ppm): 10.35 (br), 9.50 (br), 9.17 (m), 8.28 (br), 8.03 (br), 7.68−7.44 (m), 3.30 (s), 1.99 (br), 1.68 (br), 1.21 (br), 1.11 (br), 0.63 (m); $M_w = 5.0 \times 10^3$, $M_w/M_n = 3.2$.

General Procedure for Amination of N1−**N4.** Condensed trimethylamine (2 mL) was added dropwise to a solution of **N1** (50 mg) in THF (20 mL) at −78 °C. The mixture was allowed to warm to room temperature and stirred for 12 h. The precipitate was redissolved by the addition of methanol (10 mL). After the mixture was cooled to −78 °C, additional trimethylamine (2 mL) was added, and the mixture was stirred at room temperature for another 24 h. After the solvent was removed, acetone was added to precipitate **P1** as a yellow powder (44 mg, 81%). **P2**, **P3**, and **P4** were prepared using a similar procedure in yields of 85, 85, and 80%, respectively.

P1. ^{1}H NMR (400 MHz, CD_3OD, δ, ppm): 7.82−7.48 (m, 6H), 3.24 (br, 4H), 3.03 (br, 18H), 2.10 (br, 4H), 1.56 (br, 4H), 1.16 (br, 8H), 0.59 (br, 4H). ^{13}C NMR (100 MHz, CD_3OD), δ (ppm): 152.49, 152.36, 143.02, 142.29, 141.96, 141.11, 140.78, 133.22, 132.07, 131.62, 127.96, 127.45, 127.36, 127.13, 123.65, 122.84, 122.76, 122.65, 121.82, 121.79, 121.70, 121.57, 121.46, 121.25, 91.76, 67.76, 53.60, 40.85, 30.11, 26.81, 24.65, 23.63.

P2. ^{1}H NMR (500 MHz, CD_3OD, δ, ppm): 7.86−7.54 (m, 6H), 3.26 (br, 4H), 3.09 (br, 18H), 2.13 (br, 4H), 1.60 (br, 4H), 1.19 (br, 8H), 0.62 (br, 4H). ^{13}C NMR (125 MHz, CD_3OD, δ, ppm): 152.53, 141.98, 133.22, 133.20, 133.17, 132.04, 132.01, 131.61, 128.02, 127.99, 127.97, 127.46, 127.27, 127.25, 127.23, 123.61, 122.89, 121.84, 67.70, 56.65, 53.58, 40.84, 30.12, 26.80, 24.65, 23.62.

P3. ^{1}H NMR (500 MHz, CD_3OD, δ, ppm): 10.53 (s), 9.57 (s), 9.08(s), 8.45−7.35 (m), 3.31−3.23 (m), 3.08 (br), 2.14 (br), 1.58 (br), 1.19 (br), 0.61 (br).

P4. ^{1}H NMR (500 MHz, CD_3OD, δ, ppm): 10.55 (br), 9.59 (br), 9.12 (br), 8.34 (br), 8.06 (br), 7.90−7.57 (m), 3.30 (br), 3.09 (s), 2.15 (br), 1.61 (br), 1.21 (br), 0.54 (br).

Acknowledgment. We are grateful to the National University of Singapore (NUS ARF R-279-000-197-112/133, YIA R-279-000-234-123) and Singapore Ministry of Education (MOE R-279-000-255-112) for financial support.

Supporting Information Available: The absorption and emission spectra of **P3** in the presence of metal ions, except mercury(II), and the relative fluorescence intensity of **P1** versus [ion]. This material is available free of charge via the Internet at http://pubs.acs.org.

References and Notes

(1) (a) Shen, Y.; Mackey, G.; Rupcich, N.; Gloster, D.; Chiuman, W.; Li, Y.; Brennan, J. D. *Anal. Chem.* **2007**, *79*, 3494. (b) Sarzanini, C.; Mentasti, E. *J. Chromatogr., A* **1997**, *789*, 301. (c) Robards, K.; Starr, P. *Analyst* **1991**, *116*, 1247.
(2) (a) Renzoni, A.; Zino, F.; Franchi, E. *Environ. Res.* **1998**, *77*, 68. (b) Malm, O. *Environ. Res.* **1998**, *77*, 73.
(3) Grandjean, P.; Weihe, P.; White, R. F.; Debes, F. *Environ. Res.* **1998**, *77*, 165.
(4) (a) Takeuchi, T.; Morikawa, N.; Matsumoto, H.; Shiraishi, Y. *Acta Neuropathol.* **1962**, *2*, 40. (b) Matsumoto, H.; Koya, G.; Takeuchi, T. *J. Neuropathol. Exp. Neurol.* **1965**, *24*, 563.
(5) Harada, M. *Crit. Rev. Toxicol.* **1995**, *25*, 1.
(6) Karadjova, I.; Mandjukov, P.; Tsakovsky, S.; Simeonov, V.; Stratis, J.; Zahariadis, G. *J. Anal. At. Spectrom.* **1995**, *10*, 1065.
(7) Devi, R. P.; Gangaihi, T.; Naidu, G. R. K. *Anal. Chim. Acta* **1991**, *212*, 533.
(8) Hosseini, M. S.; Hashemi-Moghaddam, H. *Talanta* **2005**, *67*, 555.
(9) Ugo, P.; Mortto, L.; Bertonecll, P.; Wang, J. *Electroanalysis* **1998**, *10*, 1017.
(10) Rurack, K.; Resch-Genger, U.; Bricks, J. L.; Spieles, M. *Chem. Commun.* **2000**, 2103.
(11) (a) Kim, I.-B.; Phillips, R.; Bunz, U. H. F. *Macromolecules* **2007**, *40*, 5290. (b) Liu, S.; Fang, C.; Zhao, Q.; Fang, Q.; Huang, W. *Macromol. Rapid Commun.* **2008**, *29*, 1212.
(12) (a) Huang, C.-C.; Chang, H.-T. *Anal. Chem.* **2006**, *78*, 8332. (b) Darbha, G. K.; Ray, A.; Ray, P. C. *ACS Nano* **2007**, *1*, 208. (c) Lee, J.-S.; Mirkin, C. A. *Anal. Chem.* **2008**, *80*, 6805.
(13) (a) Winkler, J. D.; Bowen, C. M.; Michelet, V. *J. Am. Chem. Soc.* **1998**, *120*, 3237. (b) Xu, X. H.; Thundat, T. G.; Brown, G. M.; Ji, H. F. *Anal. Chem.* **2002**, *74*, 3611.
(14) Kim, I.-B.; Bunz, U. H. F. *J. Am. Chem. Soc.* **2006**, *128*, 2818.
(15) (a) Chen, A.; Sun, H. S.; Pyayt, A.; Zhang, X. Q.; Luo, J. D.; Jen, A.; Sullivan, P. A.; Elangovan, S.; Dalton, L. R.; Dinu, R.; Jin, D. L.; Huang, D. Y. *J. Phys. Chem. C* **2008**, *112*, 8072. (b) Sanchez, J. C.; DiPasquale, A. G.; Rheingold, A. L.; Trogler, W. C. *Chem. Mater.* **2007**, *19*, 6459.
(16) (a) Rininsland, F.; Xia, W. S.; Wittenburg, S.; Shi, X. B.; Stankewicz, C.; Achyuthan, K.; McBranch, D.; Whitten, D. *Proc. Natl. Acad. Sci. U.S.A.* **2004**, *101*, 15295. (b) Kumaraswamy, S.; Bergstedt, T.; Shi,

X. B.; Rininsland, F.; Kushon, S.; Xia, W. S.; Ley, K.; Achyuthan, K.; McBranch, D.; Whitten, D. *Proc. Natl. Acad. Sci. U.S.A.* **2004**, *101*, 7511.
(17) Thomas, S. W.; Joly, G. D.; Swager, T. M. *Chem. Rev.* **2007**, *107*, 1339.
(18) (a) Wang, B.; Wasielewski, M. R. *J. Am. Chem. Soc.* **1997**, *119*, 12. (b) Zhang, Y.; Murphy, C. B.; Jones, W. E., Jr. *Macromolecules* **2002**, *35*, 630.
(19) Zaporozhets, O.; Gawer, O.; Sukhan, V. *Talanta* **1998**, *46*, 1387.
(20) Ou, S. J.; Lin, Z. H.; Duan, C. Y.; Zhang, H. T.; Bai, Z. P. *Chem. Commun.* **2006**, *42*, 4392.
(21) Watanabe, S.; Seguchi, H.; Yoshida, K.; Kifune, K.; Tadaki, T.; Shiozaki, H. *Tetrahedron Lett.* **2005**, *46*, 8827.
(22) (a) Plaschke, M.; Czolk, R.; Ache, H. J. *Anal. Chim. Acta* **1995**, *304*, 107. (b) Monti, D.; Venanzi, M.; Russo, M.; Busso, M.; Bussetti, G.; Goletti, C.; Montalti, M.; Zaccheroni, N.; Prodi, L.; Rella, R.; Manera, M. G.; Mancini, G.; Di Natale, C.; Paolesse, R. *New J. Chem.* **2004**, *28*, 1123.
(23) Fang, Z.; Liu, B. *Tetrahedron Lett.* **2008**, *49*, 2311.
(24) Dolci, L. S.; Marzocchi, E.; Montalti, M.; Prodi, L.; Monti, D.; Di Natale, C.; D'Amico, A.; Paolesse, R. *Biosens. Bioelectron.* **2006**, *22*, 399.
(25) Li, B.; Li, J.; Fu, Y.; Bo, Z. *J. Am. Chem. Soc.* **2004**, *126*, 3430.
(26) Liu, B.; Gaylord, B. S.; Wang, S.; Bazan, G. C. *J. Am. Chem. Soc.* **2003**, *125*, 6705.
(27) Fang, Z.; Breslow, R. *Org. Lett.* **2006**, *8*, 251.
(28) Wang, Q. M.; Bruce, D. W. *Synlett* **1995**, 1267.
(29) Screen, T. E. O.; Thorne, J. R. G.; Denning, R. G.; Bucknall, D. G.; Anderson, H. L. *J. Mater. Chem.* **2003**, *13*, 2796.
(30) Kilian, K.; Pyrzyńska, K. *Talanta* **2003**, *60*, 669.
(31) Kano, K.; Minamizono, H.; Kitae, T.; Negi, S. *J. Phys. Chem. A* **1997**, *101*, 6118.
(32) Nielsen, K. T.; Spanggaard, H.; Krebs, F. *Macromolecules* **2005**, *38*, 1180.
(33) Kano, K.; Fukuda, K.; Wakami, H.; Nishiyabu, R.; Pasternack, R. F. *J. Am. Chem. Soc.* **2000**, *122*, 7494.
(34) Balaji, T.; Sasidharan, M.; Matsunaga, H. *Analyst* **2005**, *130*, 1162.
(35) Dolphin, D. *The Porphyrins, Volume 1, Structure and Synthesis, Part A*; Academic Press: New York, 1978.
(36) Lakowicz, J. R. *Principles of Fluorescence Spectroscopy*; Kluwer Academic/Plenum: New York, 1999.
(37) Schulman, S. G., Ed. *Molecular Luminescence Spectroscopy: Methods and Applications*; Wiley: New York, 1985.

MA801874Z